Testing And Validation Of Travelling Wave Based Fault Detection And Location Method For Offshore Wind Farm Applications

Ghosh, Sujay; Yang, Guangya; Moser, Asmus G.; Anaraki, Seyed A. H.

Published in:
Energy Reports

Link to article, DOI:
10.1016/j.egyr.2023.05.053

Publication date:
2023

Document Version
Publisher's PDF, also known as Version of record

Available online at www.sciencedirect.com
ScienceDirect
Energy Reports 9 (2023) 431–440
www.elsevier.com/locate/egyr

2022 The 3rd International Conference on Power and Electrical Engineering (ICPEE 2022)
29–31 December, Singapore

Testing and validation of travelling wave based fault detection and location method for offshore wind farm applications

Sujay Ghosh[a,*], Guangya Yang[a], Asmus G. Moser[b], Seyed A.H. Anaraki[b]

[a] *Technical University of Denmark, 2800 Kgs. Lyngby, Denmark*
[b] *Ørsted Wind Power A/S, Kraftværkvej 53, 7000 Fredericia, Denmark*

Received 17 April 2023; accepted 17 May 2023
Available online xxxx

Abstract

This work investigates the efficiency of Travelling Wave (TW) based fault detection and locationing for multi-sectional cross-bonded export cable for offshore wind farm applications. The cables, instrument transformers and the offshore wind farm are modelled according to the TW method and practical conditions. In order to correctly reflect the offshore collection grid dynamics, an aggregation method that preserves the frequency response of the wind farm impedance is implemented. The result of the EMT simulation of the developed offshore system model is played back on an actual TW relay to test the reliability of the current-based TW FDL method. A simulation of TW FDL using wavelet transform is performed to verify the relay response. Through cross-validation with the relay testing result, the paper provides another aspect of the applicability of TW relay for offshore applications.

Peer-review under responsibility of the scientific committee of the 3rd International Conference on Power and Electrical Engineering.

Keywords: Cross-bonded cable; Travelling wave; Offshore wind farm; Fault locationing; Test and validation

1. Introduction

Nowadays, offshore wind farm (OWF) is growing in size as well as the distance to shore to harvest better wind conditions in the deep sea. The majority of the wind farms use long-distance high voltage cables to export the energy from the offshore collection grid to shore. Extensive use of cables in OWFs makes a distinct difference electrically as well as in operation and maintenance from the onshore counterparts. As cable faults typically present permanent damages, onsite reparation is usually inevitable. To reduce the damage and improve the time of reparation, fast detection of the fault as well as precise locationing will help the operators to improve the safety of the assets, reduce the potential downtime due to turbine disconnection, and increase the availability of the full capacity of the wind farm.

* Corresponding author.
E-mail address: sujgh@dtu.dk (S. Ghosh).

https://doi.org/10.1016/j.egyr.2023.05.053

Peer-review under responsibility of the scientific committee of the 3rd International Conference on Power and Electrical Engineering.

In terms of export cable protection and fault locationing, commonly adopted method is still distance relay. There has been vast literature on using distance relays to detect and locate the faults on overhead lines. For OWFs, the long export cables adopt multiple sections in order to have the reach; however, due to the presence of the multiple cable junctions across the sections, the entire cable show non-homogeneous impedance characteristics, which introduces extra difficulties for the impedance-based relay to accurately locate the fault by the estimated fault impedance [1].

Dommel and Michels first proposed using travelling wave (TW) propagation to locate line faults in 1978 [2]. The technology has started to draw attention recently after the breakthrough in digital sampling and data storage technologies. The TW-based fault locationing methods, i.e. single and double-ended [3–13], applied to a hybrid transmission line have been deeply studied in the literature. In [4–6], one of the steps to locate the fault is to distinguish if the fault is on an overhead line (OHL) or cable section via polarities of first and second wavefronts. Since overhead lines and cables have different characteristics impedances, it creates a specific property for wave polarities. In [3–7], the fault location is computed without synchronised measurements and is independent of the wave velocity. This helps solve the problem of cable changing parameters due to changing relative permittivity with age. In [8], a fault location is demonstrated on a High-voltage direct current (HVDC) network with segments of cables and OHLs. Nevertheless, the studies do not take into account the detection of the transient event and the influence of the measurement dynamics.

To extract the current TW caused by a fault, Wavelet Transform analysis has been introduced and widely studied in [3–6,11] because of its high efficiency and accuracy. In [9], the Short-Time Matrix Pencil Method is used to extract the current TW and achieves the purpose of fault location. Compared with the commonly used wavelet analysis, the results show that the Short-Time Matrix Pencil method has higher feasibility and accuracy. In [10], parameter estimation from statistical theory is used to solve the redundant transmission equations formed by multiple measuring points to locate the faults. In addition, the bad data error detection capability of the parameter estimation improves locating accuracy. In [11], the authors propose a closed-form solution for two-terminal TW-based fault location on hybrid transmission lines, which considers the effects of uncertainties in line parameters, such as ambient temperature, ground characteristics, conductor features, and so on, on the estimated fault distances. In [12], the authors propose a TW fault location method based on a bi-level decision matrix (BDM) aiming at multi-branch deep-sea offshore wind farm transmission lines, where based on the fault area inherent topology and the TW arrival time, the decision matrix is built to identify fault section. The approach does not need to install recorders at all terminals, and has high fault location accuracy. In [13], new algorithms have been proposed for multi-branch hybrid transmission lines, fault locating methods based on pattern recognition techniques such as Embedded Artificial intelligence, clustering and regression algorithms. The performance of the proposed methods is tested for various fault scenarios with satisfactory results in real time. However, all the above methods proposed either have not been validated from hardware or benchmarked with actual TW relay for accuracy in terms of different configurations of the lines.

Therefore, the work in this paper first tested the efficiency of an actual TW relay tested on overhead lines for fault detection and locationing (FDL) on long radial multi-sectional and cross-bonded HV export cables used in offshore wind farms. The travelling wave is simulated based on a detailed model of the cable, instrument transformers and other substation equipment. Furthermore, the efficacy of the TW relay is compared with a Wavelet method implemented in simulation. The agreement of the results between the two platforms will provide cross-validation of both methods for their feasibility for application on the export cable of OWFs.

The contribution of the paper is summarised below,

- Tests are performed on a commercial TW relay for typical faults on offshore wind farm export cable;
- To enhance the validity of the conclusion, The paper implemented a conventional Wavelet Transform-based method to cross-validate the test results and the conclusion;

The paper is organised as follows. Section 2 presents a detailed offshore wind farm simulation model constructed in PSCAD/EMTDC compatible with TW theory. In Section 3, the reliability of the current TW-based FDL is tested for the common operation events and faults in an offshore system. Further, to verify the results of the relay testing and validate the TW concept for multi-sectional cable applications, Section 4 examines an analytical method for fault locationing based on Wavelet Transform. Finally, Section 5 presents the conclusion of the work.

2. System modelling

This section presents the key component models used in Electromagnetic Transients (EMT) simulation. The data provided here are based on manufacturers' input augmented by typical installation methods.

2.1. Multi-sectional cross-bonded high voltage export cable

A typical high voltage (HV) co-axial cable is formed by four main layers — conductor, insulation, sheath, outer insulation and sometimes armour. The cables also have semi-conductive (SC) layers, swelling tapes and metal foil. An offshore wind farm export cable is a three-phase HV co-axial cable installed in a combination of land and submarine cables.

2.1.1. Land cable

In the simulation model, the land cable construction consists of three 2000 mm^2 single-phase aluminium conductor cables, each having a rated voltage of 220 kV. The three cables are laid in a flat formation, and their screens are grounded at both terminal ends. The length of the land cable considered is 10 km (one major section of 10 km). The cables' average depth and horizontal spacings are 1.2 m and 1 m, respectively. The resistivity of the surrounding dry soil considered is 100 Ωm. Due to the confidential and sensitive nature of the key parameters given by the manufacturer for the land cable and further the submarine cable and instruments transformers, their modelling data is not presented.

2.1.2. Submarine cable

The submarine cable considered is a three-core 1200 mm^2 copper cable with a voltage rating of 220 kV. The three cables are laid in a tight trefoil formation and enclosed in a pipe (armour). The length of the cable is 100 km with the sheaths cross bonded (with 1 uH/m copper cable) using four major sections, where the length of each section is 25 km. Under normal operation, the sheath carries the charging current; hence it is grounded to avoid sheath over-voltages at cable terminals [14]. For long cables, the sheaths are cross bonded, such that the induced sheath currents cancel out. On average, the depth of the submarine cable is about 3 m under the seabed, and the resistivity of the surrounding wet soil considered is 1 Ωm. The frequency-dependent phase model of the hybrid export cable is implemented in an EMT simulation environment [15].

2.2. Instrument transformers

The frequency response of instrument transformers should be included in the travelling wave simulation to ensure realistic voltage and current inputs to the relay.

2.2.1. Current transformer

A good characterisation of the high-frequency components in the secondary side of inductive current transformers (CT) is reported in Elhaffar [16],Douglass [17],Meliopoulos et al. [18], where it is discussed that they can be used up to 200 kHz. In the present study, a wide bandwidth multi-core 10 VA 5P20 inductive CT is selected, with a ratio of 1250:1 ($N = 1250$). A CT secondary resistance of 2.5 mΩ per turn is assumed. Different parasitic components, such as magnetising inductance, leakage inductance, and stray capacitance, are considered to correctly represent the CT's bandwidth. The transformer core saturation is also implemented to study its impact on the TW-based FDL.

2.2.2. Voltage transformer

In Imris and Lehtonen [19], the inductive voltage transformer (VT) is used for transients only up to 10 kHz since the inductive voltage coupler compromises the accuracy of the fault location due to its band-pass features [20]. However, in our analysis, we still use an inductive VT. This is because a high bandwidth VT is not required since current measurements only are sufficient for the computation of fault location. We still need a VT as input to the relay in case current measurements are faulty and for the other protection functions. In this regard, an inductive VT with a 2000 ratio and 115 V operating voltage is used in the studies. Due to the unavailability of the manufacturer's real modelling data, typical VT parameters are adopted [15].

2.3. Wind turbine model

In this work, a type-4 wind turbine (WT) EMT model consisting of a Permanent Magnet Synchronous Generator (PMSG), Grid-side converter and controls (GSC), Machine-side converter and controls (MSC), AC filter with

phase reactors, DC link capacitor, DC chopper and a transformer, are considered. The details regarding the WT specifications are presented in Table 1.

Table 1. Wind turbine specifications.

Component	Modelling parameters
Permanent Magnet Synchronous Generator (PMSG)	2 MVA, 0.69 kV, 30 Hz
AC-DC-AC converter	2-level, 3-phase, IGBT-based Switching model
DC link capacitor	1400 V_{DC}, 15000 μF
DC link chopper	2 MVA, $V_{activation} = 1.05$ p.u.
Filter with phase reactor	$L_{conv} = 335$ μH, $C_{filt} = 700$ μF, $L_{damp} = 621$ μH, $C_{damp} = 700$ μF, $R_{damp} = 1.3$ Ω
WT Transformer	2 MVA, 0.69/33 kV, 50 Hz, $X_1 = 0.025$ p.u.

Two levels of hierarchy are implemented in the synchronous direct-quadrature (DQ) reference frame to incorporate the controls for both GSC and MSC. The GSC controls the voltage of the DC link capacitor and the voltage/reactive power at the AC grid bus. During fault conditions, the cascaded AC voltage and reactive power controller inject reactive power into the fault. However, the currents from the converter cannot exceed its rating; therefore, a current limiting logic is also implemented. The MSC controls the active power output from the PMSG and the AC voltage at its terminal to obtain the required ratings at the output terminal of the WT.

In the controllers, the information about the instantaneous grid voltage, phase, and frequency is obtained via the Phase-locked loop (PLL) [21], where a Synchronous Reference Frame (SRF) PLL is implemented. Further, during a fault condition, protection of the DC link capacitor is required to avoid overvoltages [22]. Therefore, the size of the chopper resistance is designed such that it can dissipate the full power rating of the WT.

2.4. Aggregated wind farm model

To test the reliability of the TW-based FDL, an offshore wind farm with 100 2MW type-4 WTs along with its associated transmission network is considered. In the offshore wind farm, each WT is connected to the Point of Connection (PoC) through a similarly low and medium voltage electrical network. At the PoC, all the WTs are linked in a series and/or parallel combination. Finally, from PoC, the aggregated power from all the WTs is exported through a HV network to the Point of Common Coupling (PCC), i.e. AC power grid.

To reduce the computational burden of the detailed EMT offshore collection grid, it can be simplified into a single-line diagram with a single-machine (WT) equivalent. The principle adopted in this paper is based on equivalenting the power losses in the medium voltage array cables and transformers. The detailed methodology for modelling the aggregated network was established in Ghosh et al. [23], where two configurations are considered, series- and parallel-connected WTs. This preserves the resonant frequencies of the whole offshore wind farm. However, if the resonant frequencies are off from the original frequency plot, then the lengths of the medium voltage (MV) cable can be tuned to obtain the desired frequency response [24]. The details regarding the offshore wind farm specifications are presented in Table 2.

Table 2. Offshore wind farm specifications.

Component	Modelling parameters
Rated capacity	100, 2 MVA units, 10 series, 10 parallel config.
MV cable (per phase/km)	33 kV, π-model, L = 0.55 mH, C = 0.26 μF, R = 0.05 Ω
Offshore Transformer	200 MVA, 33/220 kV, $X_1 = 0.02$ p.u., High-frequency model
HV export cable	Refer to Section 2.1.
AC Grid	220 kV, 3-ph, 50 Hz

2.5. EMT model assumptions

The following are some assumptions considered in the EMT modelling:

- For the high-frequency studies, the grid behind the PCC is modelled as a passive lumped equivalent network. It is considered that there is immediate connectivity with a transformer along with additional lines in parallel.
- The 50 Hz transformer model is used with a π of capacitors, used to represent the high-frequency response of the offshore transformer [25]. The values of the parasitic capacitances are taken from [26].
- The arc voltage drop in the HV export cables during faults is neglected for the TW-FDL analysis, as the arc is very short, resulting in negligible arc impedance [27].

3. Test setup and key results

Fig. 1 presents the schematic of two TW relays at the transmission cable ends connected to a local network. The EMT-simulated waveforms are pushed to the relays. For accurate fault location purposes, the commercial relay samples the measurements at 1 MHz. The setup can test both single-ended and double-ended fault location methods. Based on the high-frequency transient input, the individual relays can compute the single-ended TW-based fault location. Additionally, the presence of optic fibre enables communication, which allows results from the double-ended TW-based fault locator. The single- and double-ended TW-based fault location method is well established in the literature. It must be noted that the commercial TW-based fault locator has been developed for overhead lines and not for pure cable configuration, as in the present case study.

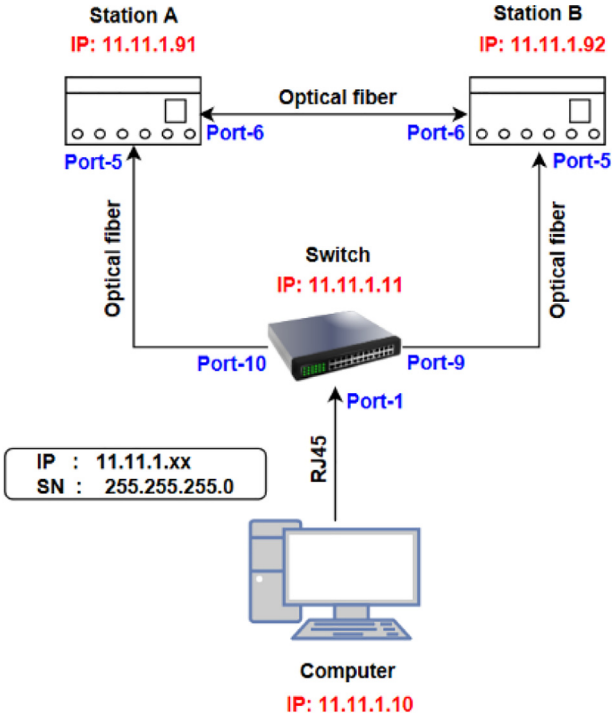

Fig. 1. Relay communication diagram.

3.1. OWF case study

When modelling the OWF single line per transformer configuration as in Fig. 2, it appears that the offshore substation's surge impedance is purely dominated by the inductance of the transformer and shunt reactor. However, it is important to note that, in reality, there is always some auxiliary system in the offshore substation that will not make the bus bar purely inductive. Hence, an additional dummy resistive load must be considered at the PoC.

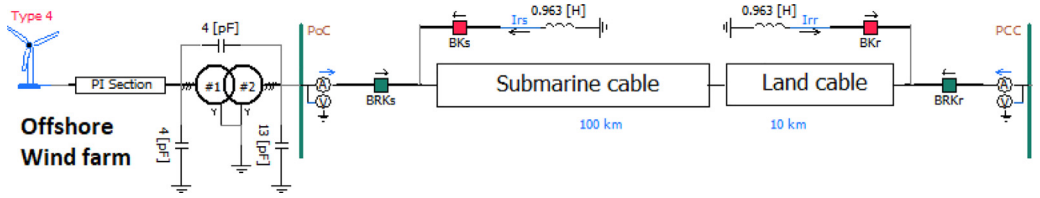

Fig. 2. Offshore wind farm with export cables.

The dummy load is an important consideration in the modelling since the current-based TW-FDL would fail for a purely inductive scenario. This is because no current can instantaneously penetrate a purely inductive winding — as the current TW meets what appears momentarily an open end, effectively reducing the wave to zero [28]. Considering the present modifications in Fig. 2, an internal cable single core to sheath (phase A) fault is applied at 35 km from PoC on the export cable. The resulting current TWs at the PoC and PCC are inspected and are presented in Fig. 3. It can be seen that both the PoC and PCC end current TWs are present; hence the fault can be accurately located by the current-based TW fault locater in the relays.

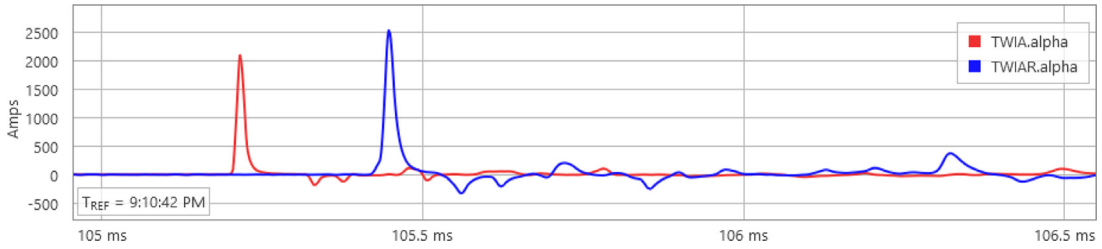

Fig. 3. PoC (red) and PCC (blue) current TW profile for a fault at 35 km on the export cable, along with transformer and a shunt reactor.

Further, the Bewley diagram for the same PoC and PCC current TW (red and blue, respectively) is represented in Fig. 4. Where it can be observed that the double-ended TW fault locator correctly identifies the necessary TWs, among many, and computes accurate fault location at 35.064 km.

In order to test the reliability of the FDL on the offshore wind farm export cable, a few other case studies are carried out, and the corresponding results are summarised in Table 3. When the fault locators' communication channel is absent or faulty, the fault location entirely depends upon the single-ended TW method. The FDL relay correctly calculates the single-ended fault location considering only the first few TWs arriving at its terminal. For a fault in a multi-sectional cross-bonded export cable, multiple TW reflections exist from the discontinuities, such as faults, bus terminals, cross-bonding, and non-homogeneous joints. Hence, an obvious drawback of this method is that if the 1st reflected wave from the fault is not among the first few TWs arriving at the terminal, this method fails. Hence, even though the current TWs at the PCC (blue) are dominant, the single-ended TW-based fault locator may not be reliable for multi-sectional cross-bonded cables; this is verified in Table 3.

Table 3. Summary of reliability study for FDL.

Description of Fault from PoC	Double ended (km)	Single-ended PoC/PCC (km)
SLG internal cable fault at 20 km	20.065	20.075/NaN
SLG cross-bonding joint fault at 25 km	25.059	25.065/NaN
LLG internal cable fault at 40 km	40.031	40.045/69.955
LLG cross-bonding joint fault at 50 km	50.012	50.025/59.975
Three-phase internal cable fault at 65 km	65.047	65.055/44.945
Three-phase cross-bonding joint fault at 75 km	75.055	75.065/34.935
SLG internal cable fault with 60° inception angle at 80 km	80.063	NaN/29.931
SLG internal cable fault with 30° inception angle at 85 km	85.067	NaN/24.927
SLG cross-bonding joint fault with saturated CT at 100 km	100.075	NaN/9.921

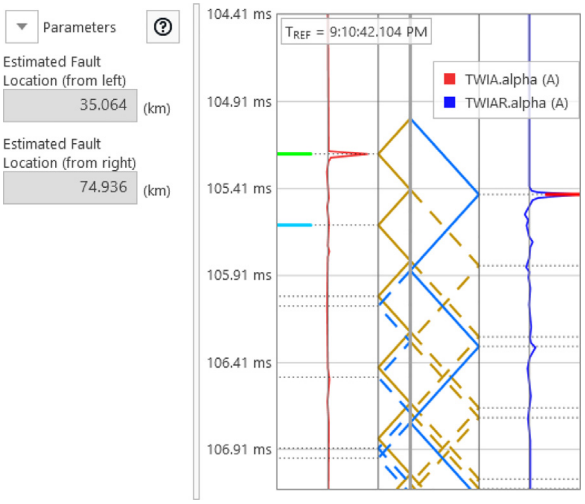

Fig. 4. Bewley's diagram for a fault at 35 km on the export cables. Red and blue legends refer to the PoC and PCC terminals, respectively. (For interpretation of the references to colour in this figure legend, the reader is referred to the web version of this article.)

An internal or joint fault in a cable occurring at peak voltage will give rise to the largest fault transient, but as the fault inception angle deviates from 90°, the magnitude of the fault voltage wave is lowered, and the TWs can be harder to pick up. However, if the pickup value of the TWs is set low enough, accurate results are expected; this is observed in Table 3. Similarly, it is also seen that the relay being an ultra-high-speed line protective relay which operates in milliseconds for line faults, the TW-FDL is not affected by CT saturation. This is because the FDL triggers within a few tenths of microseconds after the fault, whereas the core takes some time to saturate.

4. Wavelet transform and fault location

Several offline mathematical tools have been proposed in the existing literature to utilise TWs for FDL. In recent times, the Wavelet Transform (WLT) has gained a lot of popularity for solving fault location problems on overhead transmission lines. This section establishes a robust WLT-based TW-FDL algorithm that provides a second perspective on the validity of TW-FDL for offshore wind farm applications.

4.1. Wavelet transform — theory

Given a current/voltage signal *x(t)*, its continuous wavelet transform can be obtained as follows [29]:

$$WLT_{(a,b)} = \frac{1}{\sqrt{a}} \int_{-\infty}^{+\infty} x\,(t)\ \Phi^{*}(\frac{t-b}{a})dt \tag{1}$$

Where Φ is the mother wavelet offers a source function to generate daughter wavelets, which are simply the scaled *'a'* and translated *'b'* versions of the original mother wavelet. The prevalent mother wavelets used for fault location are the Morlet, the Symlet, the Daubechies, and the Haar wavelet [30].

The WLT proves useful in extracting the initial TW and the reflections from the actual current/voltage measurements. This is obtained by the modulus maxima (or the local maxima) of the WLT signal [31]. The strength and direction of the signal can be identified by the amplitude and polarity of the modulus maxima, respectively. When TWs arrive at the relay near the line terminals, the modulus maxima of the current/voltage WLT appear simultaneously.

4.2. Fault location strategy

To determine whether a current/voltage TW has arrived at a bus terminal is to examine its WLT coefficients (WCs) at its optimal scale and then compare them against a pre-determined threshold value. For WLT, different

mother wavelets will have different abilities to capture the fault TWs. Similarly, the optimal scale will depend on the unique frequency content and the noise level in the analysed signal. Therefore, the choice of mother wavelet, optimal scale, and threshold value is based on an engineering evaluation for a given system. In a real-life system, since the fault location and signal frequency content are unknown, a consolidated methodology for FDL is needed. The steps of the proposed FDL algorithm are explained as follows:

- Step-1: Simulate a cable fault and transform the phase signals (voltage and/or current) into modal components by Clark transformation.
- Step-2: Identify the fault type using the mode components
- Step-3: Calculate the WCs with all mother wavelets, i.e. Morlet, Symlet, Daubechies, and Haar wavelets at scales - 2^1, 2^2, 2^3, 2^4, 2^5, 2^6 and 2^7.
- Step-4: Compute the fault location based on all the combinations in Step 3.
- Step-5: Compare the computed fault locations in Step 4 with the actual fault location. The combination that is closest to the actual fault location is awarded a point.
- Step-6: Steps 1–5 are repeated for different types of faults at random cable locations. The combination with the highest rank (points) is considered the optimal scale and best mother wavelet for the given system.
- For a new case study, the WLT-based FDL is performed with the obtained *mother wavelet* and *scale* in Step 6.

4.3. OWF case study

Based on the fault location strategy, the mother wavelet and optimal scale for the OWF configuration in Fig. 2 were observed to be the Haar wavelet at 2^3 scale. The current TWs extracted are presented in Fig. 5.

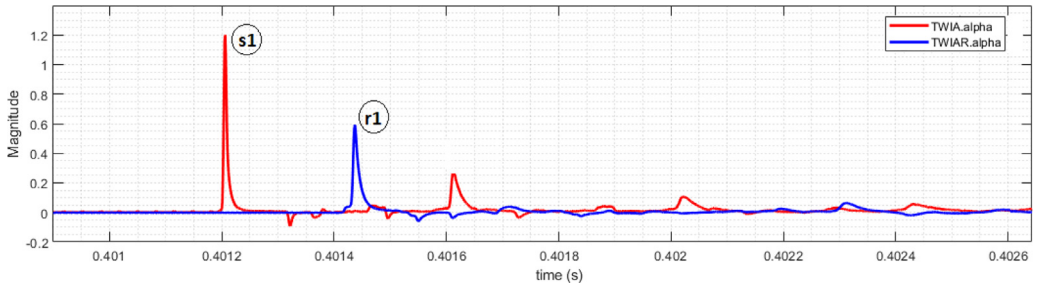

Fig. 5. Current TWs at PoC (red) and PCC (blue) for an internal fault on cable section, from WLT method (Haar, scale 2^3).

The hybrid HV export cable in Fig. 2 can be depicted as a piecewise linear characteristic, demonstrating the relationship between the distance to fault and the line propagation time to fault as in Fig. 6. Here, total line length $LL = LL_1 + LL_2$, and the total TW line propagation time $TWLPT = TWLPT_1 + TWLPT_2$. Considering $TWCT_S$ and $TWCT_R$ as the propagation delay in the CT cables at sending and receiving end, respectively; the fault location M^* (homogeneous cable) for the double-ended TW method can be computed as per,

$$M^* = \frac{LL}{2}\left(1 + \frac{(t_{s1} - TWCT_S) - (t_{r1} - TWCT_R)}{TWLPT}\right) \tag{2}$$

Further, the M^* can be corrected by projecting it onto the actual multi-sectional cable, as presented in Fig. 6. The *'M'* (double-ended fault location for actual cable) obtained is 35.084 km. It is observed that the deviation of the fault location from the WLT method is +20 m compared to the result obtained from the relay (in Section 3.1), which can be considered accurate, and hence, it can be concluded that the chosen WLT method works fine.

Further, to test the WTL-based FDL's reliability on the offshore wind farm export cable, a few other case studies are carried out, and the corresponding results are summarised in Table 4. It must be noted that since in Section 3, it was concluded that the single-ended TW method is unreliable in multi-sectional and cross-bonded cables due to multiple reflections, the results are not listed.

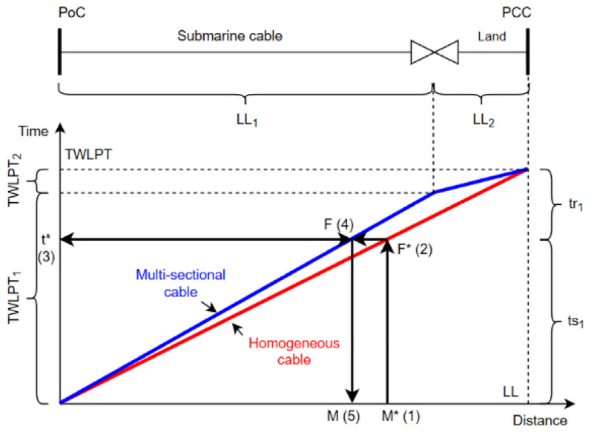

Fig. 6. Distance to propagation time characteristic.

Table 4. Summary of reliability study for WLT-based FDL.

Description of Fault from PoC	Double ended (km)
SLG internal cable fault at 20 km	20.075
SLG cross-bonding joint fault at 25 km	25.079
LLG internal cable fault at 40 km	40.061
LLG cross-bonding joint fault at 50 km	50.002
Three-phase internal cable fault at 65 km	65.067
Three-phase cross-bonding joint fault at 75 km	75.025
SLG internal cable fault with 60° inception angle at 80 km	80.023
SLG internal cable fault with 30° inception angle at 85 km	85.037
SLG cross-bonding joint fault with saturated CT at 100 km	100.045

5. Conclusion

A detailed EMT OWF was modelled, wherein the validity of the TW-based FDL was studied on its unique network configuration. When modelling the single multi-sectional cross-bonded export cable with transformer and shunt reactor termination at the offshore substation end, it is important to consider some dummy loads representing the actual auxiliary system in the offshore substation. This consideration will not make the bus bar purely inductive, which otherwise results in failure of applicability of current-based TW FDL.

The double-ended TW method provides accurate results with a maximum deviation of 75 m. Further, due to multiple TW reflections from the discontinuities such as fault, bus terminals, cross-bonding, and non-homogeneous joints, the single-ended TW method was unreliable for fault location on a multi-sectional cross-bonded cable. Further, for tests with typical fault inception angles in a cable system, the TW FDL easily picks up the TWs for fault location calculation if the pickup value is set low enough. It was also seen that the current-based TW FDL is not impacted by CT core saturation. Overall, it was observed that the robust analytical method proposed for fault detection and locating based on Wavelet transform allows accurate fault location for any network configuration and provides results similar to those obtained through the commercial relay.

Declaration of competing interest

The authors declare no conflict of interest.

Data availability

The authors do not have permission to share data.

References

[1] Das S, Santoso S, Gaikwad A, Patel M. Impedance-based fault location in transmission networks: theory and application. IEEE Access 2014;2:537–57.

[2] Glik K, Rasolomampionona DD, Kowalik R. Detection,classification and fault location in HV lines using travelling waves. Przegląd Elektrotechniczny (Electr Rev) 2012;88(1A):269–75.

[3] Qunfeng Z, Chengjun X, Hong Z. On-line fault location scheme for power cable based on arc characteristic. In: 2012 power engineering and automation conference. 2012, p. 1–4. http://dx.doi.org/10.1109/PEAM.2012.6612548.

[4] Jian Y, Zhong T. Fault location algorithm for offshore wind farm transmission cable. In: International conference on renewable power generation. 2015, p. 1–5. http://dx.doi.org/10.1049/cp.2015.0478.

[5] Altay Ö, Gürsoy E, Font A, Kalenderli Ö. Travelling wave fault location on hybrid power lines. In: 2016 IEEE international conference on high voltage engineering and application. 2016, p. 1–4. http://dx.doi.org/10.1109/ICHVE.2016.7800719.

[6] Gilany M, Ibrahim Dk, Tag Eldin ES. Traveling-wave-based fault-location scheme for multiend-aged underground cable system. IEEE Trans Power Deliv 2007;22(1):82–9. http://dx.doi.org/10.1109/TPWRD.2006.881439.

[7] He L, Wang Z, Liu H, Chen T. A double terminal traveling wave ranging method of overhead line — Submarine cable hybrid line. In: IECON 2017-43rd annual conference of the IEEE industrial electronics society. 2017, p. 16–20. http://dx.doi.org/10.1109/IECON.2017.8216007.

[8] Yang T, Gao Z, Zong P, Mu J. Hybrid line fault location method based on frequency characteristics of wave speed. In: 2020 IEEE 3rd student conference on electrical machines and systems. 2020, p. 631–5. http://dx.doi.org/10.1109/SCEMS48876.2020.9352431.

[9] Luo X, Zhang M, Wang H, Li T, Yang S. Online fault location of 110kv hybrid cable line by traveling wave based on short-time matrix pencil method. In: 2019 IEEE 8th international conference on advanced power system automation and protection. 2019, p. 289–93. http://dx.doi.org/10.1109/APAP47170.2019.9224659.

[10] Zhang K, Zhu Y, Liu X. A fault locating method for multi-branch hybrid transmission lines in wind farm based on redundancy parameter estimation. J Mod Power Syst Clean Energy 2019;7(5):1033–43.

[11] Leite EJS, Lopes FV, Costa FB, Neves WLA. Closed-form solution for traveling wave-based fault location on non-homogeneous lines. IEEE Trans Power Deliv 2019;34(3):1138–50. http://dx.doi.org/10.1109/TPWRD.2019.2900674.

[12] Wang X, Gao X, Liu Y, Wang R, Ma N, Qu M. Bi-level decision matrix based fault location method for multi-branch offshore wind farm transmission lines. Int J Electr Power Energy Syst 2022. http://dx.doi.org/10.1016/j.ijepes.2022.108137.

[13] Yan R, Geng G, Zeng G, Jiang Q and. Single-ended fault location for hybrid transmission line using embedded artificial intelligence. In: 2019 IEEE power \& energy society general meeting. 2019, p. 1–5. http://dx.doi.org/10.1109/PESGM40551.2019.8973915.

[14] Shielding Of Power Cables, https://electrical-engineering-portal.com/shielding-of-power-cables.

[15] Manitoba HVDC Research Centre Inc. Applications of PSCAD/EMTDC. Manitoba HVDC Research Centre Inc.

[16] Elhaffar AM. Power Transmission Line Fault Location Based on Current Traveling Waves [Doctoral dissertation], Helsinki University of Technology.

[17] Douglass DA. Current transformer accuracy with asymmetric and high frequency fault currents. IEEE Trans Power Appar Syst 1981;3:1006–12.

[18] Meliopoulos APS, et al. Transmission level instrument transformers and transient event recorders characterisation for harmonic measurements. IEEE Trans Power Deliv 1993;8(3):1507–17.

[19] Imris P, Lehtonen M. Modelling of a voltage transformer for transients. In: IEEE Russia power tech. 2005, p. 1–5.

[20] Spoor D, Zhu J. Transfer function analysis of coupling equipment used for traveling wave fault location. In: Proc. int. conf. electrical machines and systems. 2004.

[21] Hadjidemetriou L, Kyriakides E, Yang Y, Blaabjerg F. A synchronisation method for single-phase grid-tied inverters. IEEE Trans Power Electron 2016;31(3):2139–49.

[22] Chaudhary SK, Teodorescu R, Rodriguez P, Kjær PC. Chopper controlled resistors in VSC-HVDC transmission for WPP with full-scale converters. In: IEEE PES/IAS conference on sustainable alternative energy. 2009.

[23] Ghosh S, Kkuni KV, Yang G, Kocewiak L. Impedance scan and characterisation of type 4 wind power plants through aggregated model. In: 45th annual conference of the IEEE industrial electronics society. 2019, p. 1799–804.

[24] Pielahn M, et al. Efficient EMT modeling approach to studying resonance phenomenon in PV and wind energy systems. In: International conference on power systems transients. 2015.

[25] Greenwood A. Electrical transients in power systems. John Wiley & Sons; 2010.

[26] IEEE guide for the application of transient recovery voltage for AC high-voltage circuit breakers. 2011, IEEE Std C37.011-2011 (Revision of IEEE Std C37.011-2005).

[27] Povh D, Schmitt H, Valcker O, Wutzmann R. Modelling and analysis guidelines for very fast transients. IEEE Trans Power Deliv 1996;11(4):2028–35.

[28] Jensen CF. Online location of faults on AC cables in underground transmission systems. Springer Science \& Business Media; 2014.

[29] Mallat S, Hwang WL. Singularity detection and processing with wavelets. IEEE Trans Inform Theory 1992;38(2):617–43.

[30] Mathworks, Continuous wavelet transform.

[31] Dong XZ, et al. The application of the wavelet transform of travelling wave phenomena for transient based protection. In: International conference on power system transients. 2003.